Amphiphilic Amylose-g-poly(meth)acrylate Copolymers through "Click" onto Grafting Method

ARTICLE *in* BIOMACROMOLECULES · FEBRUARY 2011

Impact Factor: 5.75 · DOI: 10.1021/bm101143q · Source: PubMed

5 AUTHORS, INCLUDING:

Monica Bertoldo
Italian National Research Council
40 PUBLICATIONS **462** CITATIONS
SEE PROFILE

Valter Castelvetro
Università di Pisa
69 PUBLICATIONS **1,148** CITATIONS
SEE PROFILE

Amphiphilic Amylose-*g*-poly(meth)acrylate Copolymers through "Click" onto Grafting Method

Monica Bertoldo,*,† Giovanni Zampano,‡,|| Federico La Terra,† Valentina Villari,§ and Valter Castelvetro†,‡

Istituto per i Processi Chimico-Fisici, Consiglio Nazionale delle Ricerche (IPCF-CNR), Area della Ricerca, Via G. Moruzzi 1, I-56124 Pisa, Italy, Dipartimento di Chimica e Chimica Industriale, Università di Pisa, Via Risorgimento 35- I-56126 Pisa, Italy, and Istituto per i Processi Chimico-Fisici, Consiglio Nazionale delle Ricerche (IPCF-CNR), Viale Ferdinando Stagno d'Alcontres 37, 98158 Messina, Italy

Received September 23, 2010; Revised Manuscript Received November 25, 2010

Periodate oxidation and subsequent reductive amination with propargylamine was adopted for the controlled functionalization of amylose with alkyne groups, whereas ATRP polymerization was exploited to obtain end-(α)- or end-(ω)-azide functionalized poly(meth)acrylates to be used as "click" reagents in Cu(I) catalyzed azide−alkyne [3 + 2] dipolar cycloaddition. Amylose was effectively grafted with poly(*n*-butyl acrylate), poly(*n*-butyl methacrylate), poly(*n*-hexyl methacrylate), and poly(dimethylaminoethyl methacrylate) with this strategy. Their structure and composition were confirmed by FT-IR, NMR spectroscopies, and thermogravimetric analysis (TGA). Dynamic and static light scattering analyses, as well as TEM microscopy showed that the most amphiphilic among these hybrid graft copolymers self-assembled in water, yielding nanoparticles with ca. 30 nm diameter.

Introduction

Amphiphilic graft copolymers are attractive materials because they can self-assemble into nanoscale structures in solution, in bulk, and at interfaces. The micelles formed in solution have been studied as drug carriers because of their unique characteristics such as core−shell structure, mesoscopic size range, and prolonged blood circulation.[1−4] In addition, amphiphilic graft copolymers can form complex micro- and nanostructured rod-like, spheroidal, disk-like, and linelike micelles and vesicles, the actual shape depending on the interaction parameter between grafted chains and solvent. Microstructure formation and aggregate morphology stability also depend on the architecture parameters such as the position of the first graft point, the number, average length, and length distribution of branches.[5] The present application perspective of amphiphilic graft copolymers would be greatly broadened after a better understanding of such processes and correlations. Polysaccharides have been studied as surface coating materials for their biocompatibility, biodegradability, and mucoadhesive properties; they have also been considered as candidates for achieving an active targeting toward tissues and organs. With this purpose, various drug delivery systems such as liposomes and polymeric micelles have been decorated with polysaccharides.[6,7] In addition, hydrophobically modified polysaccharides self-assembling into nanoparticles have been investigated as possible drug delivery systems[8,9] exhibiting high loading efficiency as well as capability to trap and targeting the release of scarcely soluble and toxic antitumor drugs.[9] Tailor-made graft copolymers can be synthesized using specific polymerization methods mainly based on grafting "from" and grafting "to" or "onto" approches.[10,11] The grafting "from" route is the most commonly used procedure to obtain graft copolymers with controlled architecture. In this approach, the growth of copolymer grafts occurs from initiating sites on the polymer backbone (macroinitiator) by free radical, ionic, ring-opening, controlled/living radical, or even enzymatic graft copolymerization.[12−14] Conventional free radical polymerization does not allow control over grafted chain length and grafting density,[15,16] whereas ring-opening and controlled/living radical polymerization processes allow predictable molecular weight of the grafted block copolymer chains to be obtained. However, controlling the surface density of immobilized initiator and eventually the density of grafted chains can be problematic, and the result is scarcely predictable, even by these latter methods.[17]

In the grafting "onto" approach, a preformed polymer with reactive end group is coupled to functional groups along the backbone of a second polymer. When the backbone functional polymer is a polysaccharide, the nucleophilic character of its hydroxyl groups is often exploited in condensation and addition reactions.[18] By this way, cellulose-*g*-polystyrene was prepared by direct esterification of cellulose with the terminal carboxylic acid groups of well-defined polystyrene chains.[19] Cellulose substrates have been functionalized with amino groups onto which poly(isobutyl vinyl ether) and poly(2-methyl-2-oxazoline) have been grafted.[20] Similarly, poly(isobutyl vinyl ether), poly(ethylene glycol) (PEG), poly(ethyleneimine), polyurethane, poly(dimethylsiloxane), and polylactide have been grafted to chitosan[21−23] and other polysaccharides.[24−27] In most cases, these procedures are unfortunately not quantitative, resulting in low grafting densities. Furthermore, removal of the unreacted polymer may be difficult, a problem that emphasizes the need of highly efficient, high yield coupling reactions. An attractive feature of the grafting "onto" approach is that the side chains are prepared separately. This makes easily accessible such complex architectures as comb copolymers with different kinds of side chains along the backbone. With this goal, graft copolymers from functionalized PEG and guar gum have been

* To whom correspondence should be addressed. Tel: +39 050 3152230. Fax: +39 050 3152250. E-mail: monica.bertoldo@ipcf.cnr.it.
† Consiglio Nazionale delle Ricerche (IPCF-CNR), Area della Ricerca, Pisa, Italy.
‡ Università di Pisa.
§ Consiglio Nazionale delle Ricerche (IPCF-CNR), Messina, Italy.
|| Present address: A. Menarini Industrie Farmaceutiche Riunite Srl, via Marchetti 7/7 Bis, I-50131 Firenze, Italy.

10.1021/bm101143q
Published on Web 12/30/2010

recently prepared by Cu(I) catalyzed azide−alkyne [3 + 2]-dipolar cycloaddition ("click") as the coupling reaction with grafting chains.[28] The modification of galactomannans (Guar gum, Locust Bean gum, etc.) by "click" grafting "onto" with poly(oxyalkylenes) is a versatile procedure for achieving various polysaccharide-based materials.[28,29] For this purpose, alkynyl side groups have been introduced along the polysaccharide backbone by base-catalyzed etherification with propargyl bromide, targeting a broad range of substitution degrees of the pyranose ring.[30,31] Similarly, hyaluronic acid (HA) functionalized with propargylamine has been grafted by "click" coupling with azido-end-functional poly(*N*-isopropyl acrylamide) separately prepared by controlled radical polymerization.[32,33] Finally, amphiphilic chitosan graft copolymers with mixed side chains have been synthesized by "clicking" end-functional poly(ε-caprolactone) and poly(ethylene oxide) onto a polyazidated chitosan obtained by esterification with 2-bromoisobutyryl bromide, followed by nucleophilic substitution of the α-bromide with azide.[34] The effectiveness of the "click" reaction has also been demonstrated in the modification of polysaccharides by functionalization with small moieties[35−40] and cross-linking.[33,41] As already mentioned, click reactions have been combined with different controlled polymerization methods.[42] Among them, atom transfer radical polymerization (ATRP) has been extensively adopted, generating hundreds of research papers.[42−46]

In this work, amylose, an almost completely linear α-(1,4)-glucopyranoside, was modified to introduce alkynyl functionalities along the backbone and then hybridized by graft-clicking with azido-terminated (meth)acrylic homopolymers that had been obtained from end-brominated precursors prepared by ATRP.[47] The highly effective and selective "click" reaction was used to overcome the problems of low yield and selectivity frequently encountered in grafting "onto" reactions involving polysaccharides and highly hydrophobic synthetic polymers. Periodate oxidation and subsequent reductive amination was adopted for the controlled functionalization of polysaccharides with alkyne. The combination of periodate oxidation and reductive amination with either small molecule amines or polyamine has been previously exploited to obtain sponges to be used in tissue engineering,[48] or polycations for nucleic acid delivery,[49−51] and wastewater treatment.[52] Furthermore, graft and comb copolymers have been synthesized through reductive amination by exploiting polysaccharide reducing end[53−55] or, in a reverse coupling strategy, amine groups of chitosan.[22]

Finally, in this work, the self-assembling behavior in water of the hybrid graft-copolymer was investigated.

Experimental Part

Materials. Amylose (type III) from potatoes was purchased from Aldrich. Tetrahydrofuran (THF) was kept on NaOH for 24 h, then distilled (67 °C) under a nitrogen atmosphere. Sodium borate buffer (1 M, pH 8.5) was obtained by basification of a boric acid solution. The monomers (M) butyl acrylate (BA) (50 °C, 100 mmHg), butyl methacrylate (BMA) (57 °C, 18 mmHg), hexyl methacrylate (HMA) (87 °C, 18 mmHg), and dimethylaminoethyl methacrylate (DMAEMA) (82 °C, 18 mmHg) were distilled from CaH_2 under a nitrogen atmosphere. All purified solvents and chemicals were stored at low temperature (−20 °C) until use. CuBr (Aldrich, 99.999%) was stored under nitrogen and used without further purification. 1,1,4,7,10,10-Hexamethyltriethylenetetramine (HMTETA, Sigma-Aldrich, 97%). *N*,*N*,*N*′,*N*″,*N*″-pentamethyldiethylenetriamine (PMDETA, Sigma-Aldrich, 99%), ethyl-2-bromopropionate (EBP), propargylamine, and all other chemicals and solvents were used as received.

Instruments and Analysis Methods. Infrared spectra were recorded with either a Perkin-Elmer Spectrum GX or a Perkin-Elmer Spectrum One FT-IR spectrophotometer interfaced with the software Spectrum v.3.02 for data acquisition. Samples were analyzed in transmission mode as cast films on KBr windows or prepared in KBr discs. A liquid KBr cell 5×10^{-2} mm thick was used for CCl_4 solutions in the calculation of the fractional amount of N_3-end-functional polymers, df_{N3}. ^1H and ^{13}C NMR spectra were recorded with either a Varian 200 or a 300 MHz instrument from $CDCl_3$, DMSO-d_6, DMF-d_8, or D_2O solutions. Sample concentration was ∼30 mg/mL for proton and ∼60 mg/mL for ^{13}C analyses. At least 128 transients were accumulated for polysaccharide proton spectra. Thermogravimetric analyses (TGA) were carried out with a Mettler Toledo TGA/SDTA 851e instrument under 60 mL/min nitrogen flux in the 25−700 °C temperature range at a 10 °C/min heating rate on 20−30 mg samples. Elemental analyses (C, N, H) were performed on a Carlo Erba 1106 elemental analyzer. Size exclusion chromatography (SEC) analyses were carried out with a Jasco instrumental setup consisting of a PU-2089 Plus high pressure pump, RI 2031 Plus (refractive index) and UV-2077 Plus (UV) detectors, and column oven. Either two PLgel 5 μm Mixed-D columns (Polymer Laboratories) or two Ultrahydrogel Linear columns (Waters) mounted in series with guard column were used for elutions with organic and aqueous solvents, respectively. The instrument was interfaced with Borwin 1.21.61 (JMBS development) software for data acquisition and processing. Sample concentration was in the 3−5 mg/mL range, and injection volume was 20 μL for all SEC analyses. Poly(butyl acrylate) (PBA) and all polymethacrylates with the exception of poly(*N*,*N*-dimethylaminoethyl methacrylate) (PDMAEMA) were analyzed using $CHCl_3$ (1 mL/min, 40 °C) as the eluent and poly(methyl methacrylate) standards (Polymer Laboratories) for column calibration. A DMF/LiBr (1 g/L, 0.8 mL/min, 70 °C) eluent solution and polystyrene standards were used for PDMAEMA, whereas an aqueous NaCl (0.5 M)/NaN_3 (1%) eluent solution (0.5 mL/min, 40 °C) and poly(ethylene glycol)/poly(ethylene oxide) (PEG/PEO) standards (Polymer Laboratories) were used for the polysaccharides.

Flash chromatography was carried out on a Biotage ZIF-SIM FLASH instrument equipped with silica gel 60 prepacked cartridges (40 × 150 mm column, particle size 40−63 μm). Gas chromatography−mass spectrometry (GC-MS) analysis was carried out by using a Hp (Agilent) GCD series II apparatus with quadrupole analyzer.

We performed transmission electron microscopy (TEM) analysis using a Philips CM12 instrument operating at 120 keV; images were recorded with a CCD camera (Gatan 791). We prepared samples by laying drops of previously sonicated polymer dispersions over graphitized copper grids and removing excess solvent with filter paper, followed by staining with uranyl acetate (1 M in water) for 10−15 min. Finally, sample grids were washed with deionized water and dried.

Determination of aldehyde groups in oxidized polysaccharide. A modification of the procedure proposed by Zhao and Heindel was adopted.[56] In brief, the oxidized polysaccharide was dissolved (4.2 g/L) in water, the pH was adjusted to 4, then an equal amount by volume of hydroxylamine hydrochloride (2.5 M) at pH 4 was added. The mixture was stirred for 2 h and then back-titrated with NaOH 0.01 N to pH 4.

Determination of the N_3-Functionalization Degree (df_{N3}) of End-Functionalized Poly(meth)acrylates. (a) Method by FT-IR spectroscopy. Four solutions in CCl_4 containing 2-bromo-isobutyric acid 3-azidopropylester in the 3×10^{-4} to 1×10^{-3} M concentration range and poly(butyl methacrylate) (PBMA) (2.5 g/L), respectively, were cast onto KBr windows, and their FT-IR spectra were collected after solvent evaporation. The ratio between the integrals of the absorption bands at 2100 (N_3 stretching) and 1066 cm^{-1} (C−O stretching from PBMA) plotted against the N_3/PBMA mol/g ratio gave a linear plot that was fitted with a straight line ($y = 0.004 + 1920x$; $R^2 = 0.99945$) used for calibration. A mathematical deconvolution procedure was adopted to evaluate the integral of the PBMA band separately from the contribution of other partially superimposed absorptions. Seven Lorentzian functions with maxima at 1179.6, 1154.2, 1143.2, 1124.6, 1066.1, 1022.6, and 996.1 cm^{-1} were used to fit the spectra in the 1215−990 cm^{-1} range. The corresponding area ratio in the FT-IR spectrum of the functionalized

Table 1. Synthesis of Poly(meth)acrylates through ATRP: Feed Composition and Experimental Results

sample	M/I[a]	M:I:CuBr:$CuBr_2$:ligand[b]	$\bar{M}_n^{th}$ (g mol^{-1})[c]	$\bar{M}_n^{SEC}$ (g mol^{-1})[d]	$(\bar{M}_w)/(\bar{M}_n)$	conv. (%)[e]	df_{N3} (mol %)[f]
PBA	BA/EBP	45:1:0.15:0:0.15	5800	6350	1.20[3]	90	
PBA-N_3			5800	6350	1.20[3]		~100
PBMA	BMA/EBP	50:1:0.9:0.1:2	5700	6100	1.30	80	
PBMA-N_3-A	BMA/BiBAP	50:1:0.9:0.1:2	6150	6600	1.20	87	73
PBMA-N_3−B	BMA/BiBAP	49:1:1:0:1	5700	8500	1.26	81	95
PHMA-N_3-A	HMA/BiBAP	42:1:0.9:0.1:2	5350	8200	1.25	74	59
PHMA-N_3−B	HMA/BiBAP	41:1:1:0:2	5450	7400	1.19	78	94
PDMAEMA	DMAEMA/EBP	32:1:0.9:0.1:2	5030	12 600[3]	1.19	>95	
PDMAEMA-N_3	DMAEMA/BiBAP	32:1:0.9:0.1:2	5030	15 750[3]	1.34	>95	85

[a] M = monomer; I = initiator; EBP = ethyl-2-bromopropionate; BiBAP = bromo-isobutyric acid 3-azidopropylester. [b] Mole ratio; the ligand was either HMTETA or PMDETA. [c] M_n^{th} = conversion × $[M]_0/[I]_0$. [d] Average molecular weight obtained by SEC analysis; column calibration performed with either PS or PMMA standards. (See the Experimental Part.) [e] Conv. (%): monomer conversion. [f] Degree of end-functionalization of the polymer chains calculated by ^{1}H NMR. The df_{N3} values determined by FTIR for PBA-N_3 and PBMA-N_3 matched exactly those obtained by ^{1}H NMR. (See the Experimental Part.)

Table 2. Experimental Conditions and Results of Grafting "Onto" Experiments Carried out on Am-PA with N_3-Functionalized Poly(meth)acrylates (Z-N_3)

sample	Z-N3	DMSO/DMF vol/vol	N_3/alkyne (mol/mol)	T (°C)	concentration (g/L) Am-PA	concentration (g/L) Z-N_3	grafted chains (wt %)[a]	grafting yield (wt %)[b]
blank	PBA	7/12		60	13	9	<1	<3
AmBA	PBA-N_3	7/12	0.33	40−60[c]	13	9	39	95
AmBMA	PBMA-N_3-A	1/3	0.83	40−60[c]	36	74	52	91
AmBMA2	PBMA-N_3-A	0/1	0.91	40	10	20	37	63
AmHMA	PHMA-N_3-A	2/7	0.66	60	27	70	31	52
AmDMAE	PDMAEMA-N_3	5/2	0.33	40−60[c]	25	29	80	~100

[a] Calculated from TGA as [(synthetic polymer)/(polysaccharide-*g*-synthetic polymer)] × 100. [b] [(Synthetic polymer/polysaccharide)$_{TGA}$/(synthetic polymer/polysaccharide)$_{feed}$] × 100. [c] 60 °C for 5 h (24 h for AmBMA), then 40 °C.

polymer afforded the functionalization degree expressed as mol/g, which was converted to a mol/mol ratio by using the average $\bar{M}_n$ value determined by SEC (Table 1). Similarly, ethyl-2-azidobutyrate (see Supporting Information for the synthesis details) and PBA were used to build the calibration plot for calculating df_{N3} of PBA-N_3. In this case, the FT-IR spectra were collected from liquid samples, and the integral of the N_3 stretching band at 2110 cm^{-1} was plotted versus azide concentration. The linear fit of the experimental values afforded the following equation: $y = 0.04 + 0.116x$ ($R^2 = 0.9995$).

(b) Method by ^{1}H NMR spectroscopy. The functionalization degree, df_{N3}, was calculated from the ratio between the integral of the CH_2-N_3 resonance at ~3.4 ppm and that of the OCH_2 resonance at ~3.9 ppm due to the polymer side chains. The $\bar{M}_n$ values determined by SEC (Table 1) were used to convert df_{N3} from mol/g to mol/mol.

Light Scattering Measurements. The dependence of dynamic and static light scattering on the scattering angle (from 20 to 150°) was investigated with a homemade apparatus by using a He−Ne laser source at $\lambda = 633$ nm with a power of 10 mW, linearly polarized orthogonal to the scattering plane, and a computer-controlled goniometer.[57] The scattered light was collected in a pseudo-cross-correlation mode through two cooled R943-02 photomultipliers at the same scattering angle,[58] and a MALVERN 4700 correlator was used to build up the normalized intensity autocorrelation function. Amylose-*g*-PBMA (AmBMA, Table 2) solutions were investigated before and after filtering through 0.45 and 0.2 μm cellulose acetate filters, respectively, the aqueous solutions obtained after dialysis of the original 2 or 20 g/L DMSO solutions. The temperature was set at 25 ± 0.01 °C. A reference sample obtained by dialyzing pure DMSO against deionized water was also measured for comparison.

Details of the data analysis procedure can be found in the Supporting Information.

Comparative dynamic light scattering (DLS) measurements on amylose-*g*-PBMA, amylose-*g*-PBA, and amylose-*g*-poly(hexyl methacrylate) (AmBMA, AmBA, AmHMA, Table 2) were carried out at 25 ± 0.1 °C with a Brookhaven 90 Plus instrument collecting the scattered light at 90°. The results of 2 runs of 10 min accumulation each were averaged. Amylose copolymer dispersions were obtained from DMSO solutions (20 and 2 g/L), filtered (0.45 μm PTFE), diluted 1:16 with ultrapure water, and dialyzed against water for 2 to 3 days. Samples were sonicated for 1.5 h before analysis. Centrifuged samples were analyzed after processing at 4400 RCF for 10 min, whereas filtered samples were processed through 0.45 μm cellulose acetate syringe filters just before analysis. Cumulant analysis was used to obtain the average particle size and size distribution from the autocorrelation function.

Preparation of α-N_3-Poly(butyl acrylate) by Successive ATRP and Bromide-Substitution. A mixture of butyl acrylate (20 mL, 139.5 mmol) and PMDETA (97 μL) was degassed by three freeze−pump−thaw cycles; then, CuBr (66.7 mg, 0.465 mmol) was added under nitrogen. The catalyst was dissolved at 25−30 °C under stirring; then, the temperature was raised to 40 °C, and EBP (430 μL) was added to start the polymerization. The polymerization was carried out for 4 h, then stopped by exposing the mixture to air and adding THF (20 mL). The catalyst was removed by eluting with THF through a column packed with aluminum oxide. The polymer (PBA) was recovered after solvent and residual monomer evaporation.

PBA (16.2 g) was dissolved in DMF (60 mL) at 30 °C, and NaN_3 (220 mg, 3.41 mmol) was added under stirring. After 5 h, the mixture was diluted with THF and eluted through an aluminum oxide column, yielding 15.0 g of PBA-N_3 after solvent evaporation. **FT-IR** (KBr window, cm^{-1}): *PBA*: 2800−3000 (ν, C−H); 1732 (ν, C═O), 1450 (δ_a, CH_2), 1380 (δ_a, CH_3), 1160 (ν, C−O). *PBA-N_3:* 2800−3000 (ν, C−H); 2110 (ν, N_3), 1732 (ν, C═O), 1450 (δ_a, CH_2), 1380 (δ_a, CH_3), 1160 (ν, C−O). **^{1}H NMR** 300 MHz ($CDCl_3$, δ): *PBA*: 0.96 (t, CH_3, 3H), 1.38 (m, CH_2, 2H), 1.61 (m, CH_2, 2H), 1.05−2.40 (m, CH and CH_2 main chain) 4.05 (t, OCH_2, 2H). *PBA-N_3*: 0.96 (t, CH_3, 3H), 1.38 (m, CH_2, 2H), 1.61 (m, CH_2, 2H), 1.05−2.40 (m, CH and CH_2 main chain) 4.05 (t, OCH_2, 2H).

Preparation of ω-N_3-Poly(methacrylate)s by ATRP. A mixture of the given methacrylate in THF (1:1 v/v) and HMTETA was degassed by three freeze−pump−thaw cycles, then CuBr (and eventually $CuBr_2$, see Table 1) was added under nitrogen. After dissolution of the copper salt by stirring at 25−30 °C, the temperature was raised to 40 °C, and the polymerization was started by the addition of either bromo-isobutyric acid 3-azidopropylester (BiBAP; see the Supporting Information for the synthesis details) or EBP as the initiator. We stopped the polymerization after 3 h by exposing the mixture to air and adding THF. The catalyst was removed by eluting with THF through an aluminum oxide column. The polymer was recovered after solvent and

Scheme 1. Preparation of Amylose-Based Nanoparticles: Synthesis and Self-Assembling Procedures

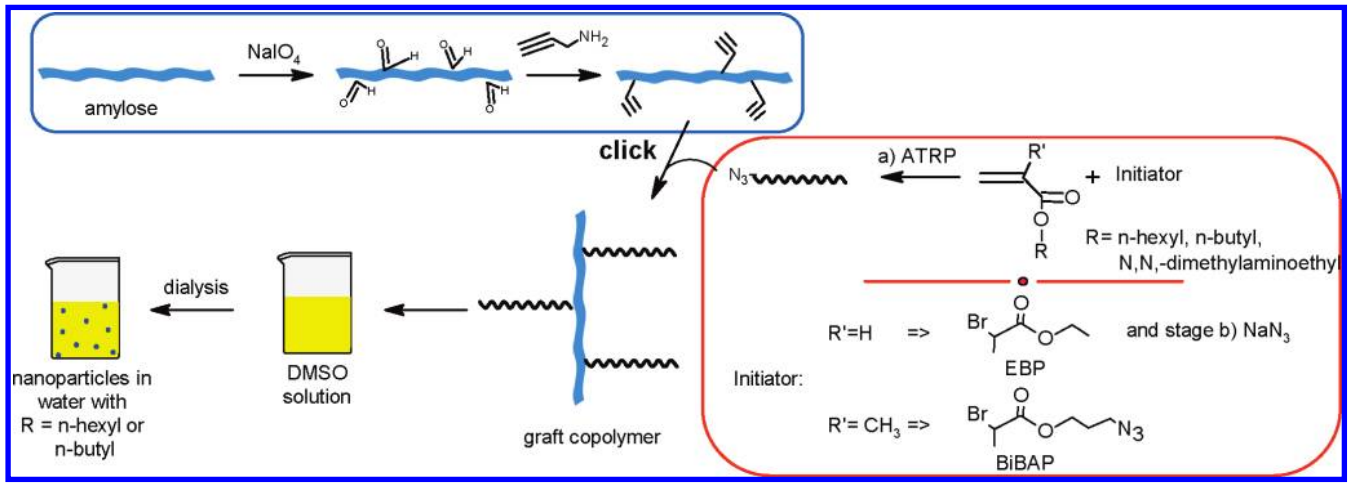

residual monomer evaporation, except for the end-functionalized PBMA−N_3−B and PHMA−N_3−B (PBMA: butyl methacrylate homopolymer; PHMA: hexyl methacrylate homopolymer), which were precipitated in MeOH at −78 °C (acetone/dry CO_2 bath), and PDMAEMAs, precipitated in cyclohexane at 0 °C (ice bath). **FT-IR** (KBr window, cm^{-1}): *PBMA-N_3*: 2850−3000 (ν, C−H), 2099 (ν, N_3), 1732 (ν, C═O), 1471, 1456 (δ_a, CH_2), 1386 (δ_a, CH_3), 1153 (ν, C−O). *PHMA-N_3*: 2850−3435 (ν, C−H), 2098 (ν, N_3), 1732 (ν, C═O), 1469, 1456 (δ_a, CH_2), 1380 (δ_a, CH_3), 1149 (ν, C−O). **^{1}H NMR** 300 MHz ($CDCl_3$, δ): *PBMA-N_3*: 0.85−1.02 (CH_3, 6H), 1.20 −1.85 (CH_2, 6H), 3.35 (t, CH_2−N_3), 4.14 (m, H_3C−O). *PBMA:* 0.85−1.02 (CH_3, 6H), 1.20−1.85 (CH_2), 4.14 (m, H_3C−O). *PHMA-N_3:* 0.88−1.01 (CH_3, 6H), 1.18−1.89 (CH_2, 10H), 3.38 (t, CH_2−N_3), 4.1 (OCH_2). *PDMAEMA:* 0.85−1.02 (CH_3, 6H), 2.25 (H_3C−N, 6H), 2.62 (CH_2), 4.15 (OCH_2). *PDMAEMA-N_3*. 0.85−1.02 (CH_3, 6H), 2.25 (H_3C−N, 6H), 2.62 (CH_2), 3.4 (CH_2–N_3), 4.15 (OCH_2).

Preparation of Alkynyl-Functionalized Amylose (Am-PA). Amylose (9.07 g, including a 10 wt % of absorbed water and butanol according to the results of TGA analysis) was dispersed in H_2O (∼35 g/L) under stirring at room temperature; then, sodium periodate (0.359 g, 0.04 mol/glucosidic unit) was added, and the solution was stirred in the dark for 2 h. The oxidized polysaccharide (Aox) was dialyzed against water (molecular weight cutoff MWCO = 2000) for 3 days and then either freeze-dried to constant weight or precipitated in ethanol, filtered, and dried under reduced pressure. Aox (4 g) was dispersed in 85 mL of aqueous borate buffer (pH 8.5) at room temperature; then, the temperature was raised to 40 °C before propargylamine (0.18 g) and $NaCNBH_3$ (0.27 g) were added. After stirring for 24 h, the reaction mixture was cooled to room temperature and the product (Am-PA) was filtered and washed with a sequence of water, acetone, and diethyl ether, then dried to constant weight. **^{1}H NMR** 300 MHz (DMSO-d_6, δ): 3.36 (H-2, H-4), 3.55−3.63 (H-3, H-6), 4.56 (OH), 4.85 (H-1 β), 5.08 (OH), 5.49 (OH). Elemental analysis (wt %): C, 40.45; N, 0.39; H, 6.26.

Preparation of Graft Copolymers by "Click" Reaction. The alkynyl-functionalized amylose (Am-PA) and the given N_3-end-functionalized poly(meth)acrylate (Table 2) were separately dissolved in DMSO or DMF at 40 °C under stirring and deoxygenated by either purging with nitrogen for 2 h or degassing through three freeze−pump−thaw cycles. DMSO was used as the solvent for amylose, except in the AmBMA2 synthesis (Table 2) that was performed in DMF. The two solutions were mixed; then, the catalyst (CuBr/PMDETA, equimolar to-N_3) and freshly prepared aqueous sodium ascorbate (4 M solution, equimolar to CuBr) were added to start the reaction that was carried out for 3 days (except AmHMA 6 days) at either 40 or 60 °C (Table 2) under a nitrogen atmosphere. Catalyst removal and solvent replacement were achieved by dialysing (MCWO = 2000) against water for 3 days. Mixtures rich in DMF were diluted with pure water before dialysis. The aqueous dispersions were centrifuged, and the collected solid was washed sequentially with water, acetone, and diethyl ether (three cycles for each solvent) to remove any unbound polymer. In the case of AmDMAE, the dialysis was carried out against an acetate buffer for 3 days, then against water for 7 days to remove catalyst and unreacted polymer. The collected solids were dried at 40 °C overnight and then under reduced pressure to constant weight. The adopted purification procedures allowed quantitative recovery of the grafted copolymer except for AmHMA, which scantily precipitated under any experimented conditions. Accordingly, FT-IR analysis of the washing solvent showed no detectable characteristic polysaccharide stretching band except for the PHMA derivative. **FT-IR** (KBr discs, cm^{-1}): *AmBA*: 3435 (ν, O−H), 2959, 2934 (ν, C−H), 1731 (ν, C═O), 1459 (δ_a, CH_2), 1155 (νa, C−C−O), 1080 (ν,C−C−O), ∼1000 (ν, C−C). *AmBM:* 3421 (ν, O−H), 1731 (ν, C═O), 1459 (ν, C−H), 1155 (ν_a, C−C−O), 1080 (ν,C−C−O), ∼1000 (ν, C−C). *AmBMA*: 3421 (ν, O−H), 2959, 2934 (ν, C−H), 1731 (ν, C═O), 1459 (δ_a, CH_2), 1155 (ν_a, C−C−O), 1080 (ν,C−C−O), ∼1000 (ν, C−C). *AmHMA:* 3420 (ν, O−H), 2930 (ν, C−H), 1731 (ν, C═O), 1459 (δ_a, CH_2), 1155 (ν_a, C−C−O), 1080 (ν, C−C−O), ∼1000 (ν, C−C). **^{1}H NMR** 300 MHz (DMSO-d_6, δ):[59] *AmBMA2:* 0.77−1.07 (CH_3), 1.37 (CH_2), 1.53 (CH_2), 3.38 (H-2, H-4), 3.62 (H-3,H-5, H-6a,b), 3.88 (OCH_2), 4.57 (OH), 5.09 (H-1), 5.38 (OH), 5.49 (OH). *AmBMA* (*room temperature*)*:* 0.79−1.08 (CH_3, CH_2 main chain), 1.36 (CH_2 side chain), 1.55 (CH_2 side chain), 3.25 (H-2, H-4), 3.65 (H-3, H-5, H-6a,b), 3.86 (OCH_2), 4.46 (OH), 5.09 (H-1), 5.30 (OH), 5.35 (OH). *AmBMA* (*60 °C*)*:* 0.79−0.91 (CH_3, CH_2 main chain), 1.37 (CH_2), 1.54 (CH_2), 3.15 (H-2, H-4), 3.34 (H_2O traces), 3.59 (H-5), 3.65 (H-3, H-6a,b), 3.89 (O−CH_2), 4.34 (OH), 5.10 (H-1), 5.21 (2OH). *AmBMA* (*80 °C*)*:* 0.79−1.08 (CH_3, CH_2 main chain), 1.39 (CH_2), 1.59 (CH_2), 3.13 (H-2, H-4), 3.32 (H_2O traces), 3.58 (H-5), 3.63 (H-3, H-6), 3.91 (OCH_2), 4.23 (OH), 5.10 (H-1), 5.23 (2OH), 7.86 (H, triazole). *AmHMA (room temperature)*: 0.74−1.08 (CH_3, CH_2 main chain), 1.28−1.62 (CH_2, 8H), 3.33 (H-2, H-4, H_2O traces), 3.62 (H-3, H-5, H-6a,b), 3.88 (OCH_2, partly overlapped), 4.56 (OH), 5.08 (H-1), 5.38 (OH), 5.48 (OH). *AmHMA* (*60 °C*): 0.78−0.98 (CH_3, CH_2 main chain), 1.30−1.85 (CH_2, 8H), 3.16 (H-2, H-4), 3.33 (H_2O), 3.64 (H-3, H-5, H-6a,b), 3.91 (OCH_2), 4.35 (OH), 5.10 (H-1), 5.21 (2OH). *AmBA* (*room temperature*): 0.88 (CH_3), 1.3 (CH_2), 1.5 (CH_2), 1.5−2.2 (CH and CH_2 main chain), 3.2−3.4 (H-2, H-4), 3.45 −3.7 (H-3, H-5, H-6a,b), 3.96 (OCH_2), 4.8 (OH), 5.1 (H-1), 5.35 (OH), 5.45 (OH), 7.95 (H triazole). *AmDMAE* (*60 °C*): 1.65−1.9 (CH and CH_2 main chain), 2.2 (NCH_3, 6H), 2.5 (CH_2N, DMSO-d_5−H), 3.25−3.4 (H-2, H-4), 3.51−3.62 (H-3, H-5, H-6a,b), 3.98 (OCH_2), 4.4 (OH), 5.12 (H-1), 5.25 (OH), 8.2 (H, triazole).

Results and Discussion

A new strategy to prepare self-assembling amphiphilic graft copolymers based on a grafting "onto" approach was adopted

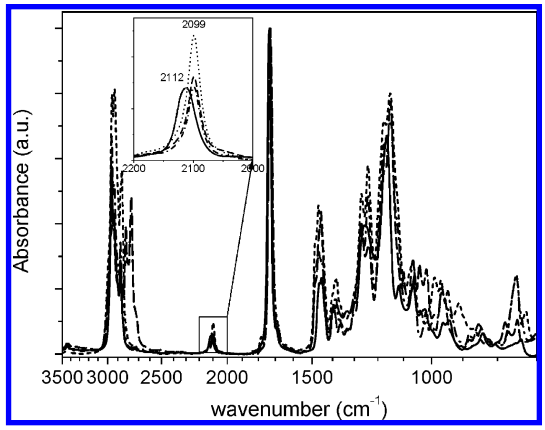

Figure 1. FT-IR spectra of N_3-end-functionalized polymers (pellets in KBr): PBA-N_3 (solid), PBMA-N_3 (dashed-dotted), PHMA-N_3 (dotted), PDMAEM-N_3 (dashed). (See Table 1.)

Scheme 2. Synthesis of 2-Bromo-isobutyric Acid 3-Azidopropylester (BiBAP)[61,62]

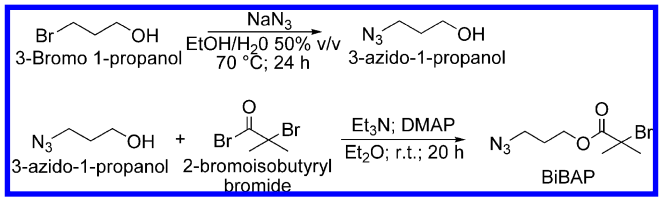

(Scheme 1). The convergent synthetic design is based on the combination of two independent reaction routes providing each a "click" reagent, namely, an alkynyl-functionalized amylose and an N_3-end-functionalized poly(meth)acrylate. These reagents are then combined under "click" conditions to give graft copolymers.

Preparation of α-N_3- and ω-N_3-End-Functionalized Poly(meth)acrylates by ATRP. The polymerization of butyl acrylate under ATRP conditions with EBP as the initiator (I) afforded Br-terminated PBA that was converted to PBA-N_3 through a nucleophilic substitution of the terminal bromide with the azide group of NaN_3.[60] The N_3 stretching band at 2112 cm^{-1} in the FT-IR spectrum of PBA-N_3 (Figure 1) was used to evaluate the degree of ω-N_3 end-functionalization (df_{N3}, Table 1) which resulted quantitative.

Unlike in poly(acrylate)s, HBr elimination leading to an α−β-unsaturated ester chain end is expected to compete effectively with bromine substitution at the tertiary carbon of end-functionalized poly(methacrylate)s. To prevent the possible generation of unreactive chain ends by such side reaction, the functional ATRP initiator 2-bromo-isobutyric acid 3-azidopropylester (BiBAP) was synthesized (Scheme 2)[61,62] and used instead of EBP in the polymerization of methacrylates, yielding α-N_3-ω-Br-functionalized polymethacrylates. Comparative experiments with EBP and the functional BiBAP initiators led to comparable monomer conversions (by NMR analysis), molecular weights, and molecular weight distributions (by SEC analysis) (Table 1). Therefore, the absence of interference of the azido group in the ATRP reaction was confirmed.

The FT-IR spectra of purified methacrylic polymers obtained with BIBAP as the initiator present the N_3 stretching band at 2099 cm^{-1} (Figure 1), from which the end-functionalization degree (df_{N3}) was determined as 73 and 95 mol % for the polymers purified by prolonged vacuum drying (sample names with suffix A, Table 1) and precipitated at low temperature (suffix B), respectively. The ^1H NMR results (Figure 2) confirmed the df_{N3} values obtained by FT-IR. In the case of

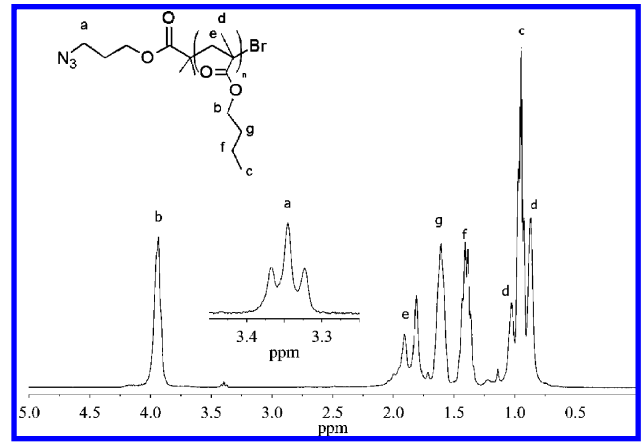

Figure 2. ^1H NMR (300 MHz, $CDCl_3$) spectrum of PBMA-N_3-B.

Scheme 3. Amylose Functionalization with Alkynyl Groups by a Two-Step Procedure: Oxidation by Periodate and Successive Reductive Amination with Propargylamine

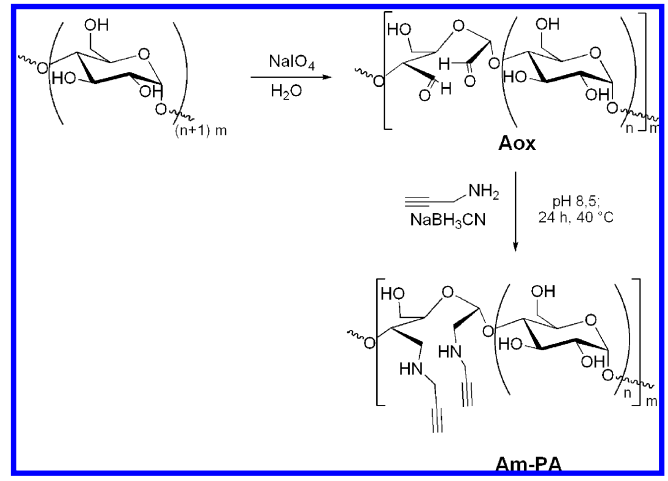

PHMA-N_3 and PDMAEMA-N_3, the df_{N3} values were similar to that of PBMA-N_3 after analogous purification process (samples A and B). The lowest df_{N3} value (59 mol %) was obtained for PHMA-N_3, possibly as a result of some photocleavage occurring while drying in vacuum the reaction product contained in a glass flask in the 40−80 °C temperature range, without protection from environmental light. In the case of PDMAEMA-N_3 precipitated at 0 °C, the comparatively lower df_{N3} value (85 mol %) is likely to be the result of an overestimation of the PDMAEMA molecular weight from SEC with calibration performed using PS standards, in agreement with the findings of Lowe et al.[63]

Functionalization of Amylose with Alkynyl Groups. A two-step procedure was adopted to functionalize amylose with alkynyl groups: initial oxidation by periodate afforded aldehyde groups (Aox) which were then modified by reductive amination with propargylamine (Am-PA) (Scheme 3). Periodate oxidation quantitatively afforded 8 mol % of aldehyde groups per pyranose ring (df = 8.2 mol %, Table 3), as determined by titration with hydroxylamine hydrochloride. (See the Experimental Part.)

The reaction of Aox with propargylamine in the presence of $NaCNBH_3$ at pH 8.5 afforded Am-PA. Preferential conversion of the intermediate imine to amino groups with respect to the competitive aldehyde reduction to hydroxyl groups is achieved under alkaline conditions,[64] the latter also being effective in catalyzing the back reaction of hemiacetals to aldehyde, thus increasing the final amination yield. Indeed, a comparative reaction performed at pH 5 resulted in degradation of the

Table 3. Functionalization Degree and Average Molecular Weight by SEC (H_2O/NaCl) Analysis of Oxidized (Aox) and Alkynyl-Functionalized (Am-PA) Amylose

sample	*df* (% mol/mol)[a]	propargylation yield (% mol/mol)[b]	$\bar{M}_n$ (g mol^{-1})	$(\bar{M}_w)/(\bar{M}_n)$
amylose			19 800[c]	1.6
Aox	8.2		9700	1.5
Am-PA[d]	4.6 ± 0.7	56 ± 9	13 300	1.4

[a] Aldehyde/pyranose ring or alkyne/pyranose ring × 100. [b] $df_{alkyne} \times 100/df_{aldehyde}$. [c] Possible overestimation due to the presence of aggregates, as suggested by the bimodal profile of the SEC trace. [d] Average value from three experiments.

Scheme 4. Synthesis of Amylose-*g*-PBA Copolymers by "Click" Grafting onto Reaction

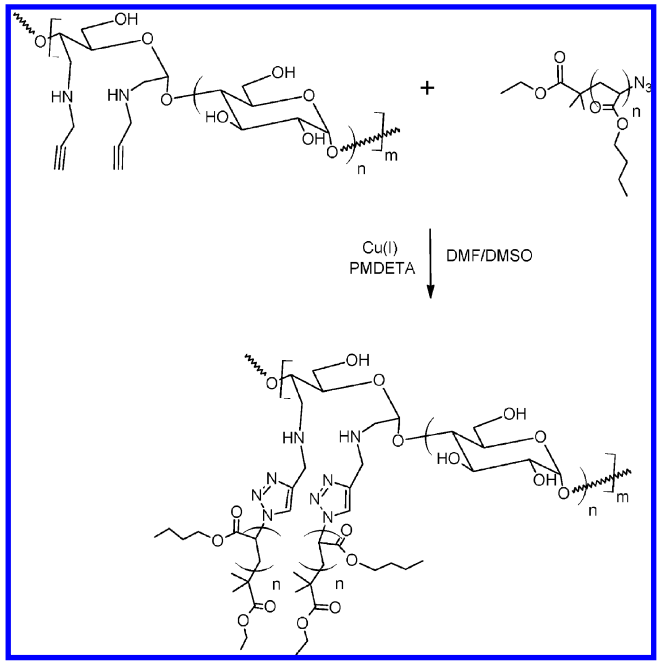

polysaccharide chain and no detectable amination. From the nitrogen content of Am-PA determined by elemental analysis, a 4.6 ± 0.7 mol % alkynyl functionalization degree (*df*, Table 3) was determined, corresponding to a 56% aldehyde conversion, slightly lower than the typical 70−80% conversions reported for the reductive amination of low-molecular-weight aldehydes.[64] The molecular weight of the polymer after functionalization with propargylamine (Am-PA) by reductive amination was comparable to that of the oxidized precursor (Aox) (Table 3), once considering the $\bar{M}_n$ increase caused by the grafted propargylamine.

Preparation of Amylose-*g*-poly(meth)acrylate Copolymers by "Click" Reactions. The alkynyl-functionalized amylose (Am-PA) was used for grafting "onto" reactions with the N_3-end-functionalized poly(butyl acrylate) (PBA-N_3) by the "click" Cu(I)-catalyzed [3 + 2] dipolar cycloaddition (Scheme 4).[65] The reaction was carried out using an equimolar amount of catalyst with respect to the alkynyl groups in homogeneous phase by DMSO/DMF mixed solvent (Table 2) because DMSO is a good solvent for amylose and DMF is a solvent of polymethacrylates that does not precipitate the polysaccharide. The reaction temperature was initially set to 60 °C to improve the reagent solubility. The ^{1}H NMR and FT-IR spectra of the reaction products obtained under such conditions presented the characteristic features of both the synthetic polymer and the polysaccharide (Figures 3 and 4). In particular, in the ^{1}H NMR spectra

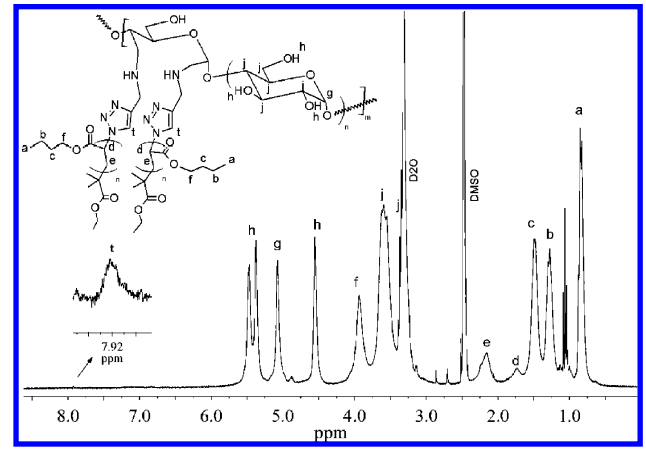

Figure 3. ^{1}H NMR (300 MHz, DMSO-d_6, 25 °C) of the AmBA graft copolymer.

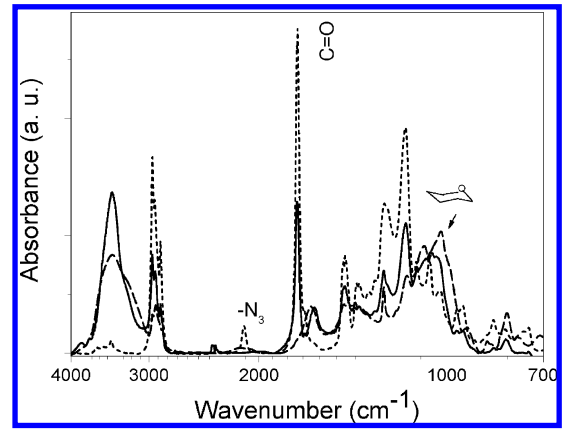

Figure 4. FT-IR of PBA-N_3 (dotted), Am-PA (dashed), and AmBA (solid line). Films cast on KBr disks.

of the graft copolymers, both the CH_3 and CH_2 proton resonances from the PBA chains in the 0.5−2.5 ppm range and those of the amylose protons in the 3−6 ppm range are present (Figure 3). Accordingly, in the FT-IR spectrum, both the characteristic C═O stretching band of polyacrylates at 1732 cm^{-1} and the typical C−C complex stretching band of the pyranose ring centered at 1022 cm^{-1} (Figure 4) are present. The complete disappearance of the N_3 stretching band at 2112 cm^{-1} in the FT-IR spectrum and the appearance of a ^{1}H NMR resonance at 7.9 ppm due to the triazole ring proton proved the formation of the amylose-*g*-PBA copolymer (AmBA) by azide−alkyne cycloaddition.

When PBA without azide functionality was used (blank, Table 3), only negligible traces of polymer were collected after purification by subsequent washings with the solvents for the homopolymers, the residual solid being PBA according to the NMR and FT-IR spectra. Therefore, the effectiveness of the purification procedure to remove possible unbound polymers was confirmed, and the occurrence of any grafting reactions by a mechanism different from the azide−alkyne cycloaddition could be excluded. Furthermore, the polysaccharide recovered from the solvent extracts had a SEC M_n = 13 900 Da, practically the same as the unprocessed Am-PA, confirming that no polysaccharide degradation occurs under the adopted "click" reaction conditions. Such inertness of polysaccharide chains had been already observed by some of the authors of this work for the chitosan azide/alkyne click functionalization in DMF under oxygen-free conditions.[41]

The adopted reaction conditions had been previously optimized in DMF, a single solvent homogeneous phase, by using

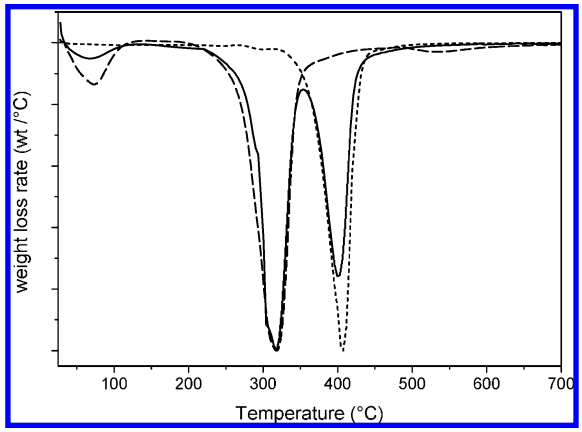

Figure 5. Weight loss rate (first derivative of the TGA weight loss curve) for the AmBA graft copolymer (solid line), the parent ungrafted Am-PA (dashed line), and the grafting PBA-N_3 (dotted line).

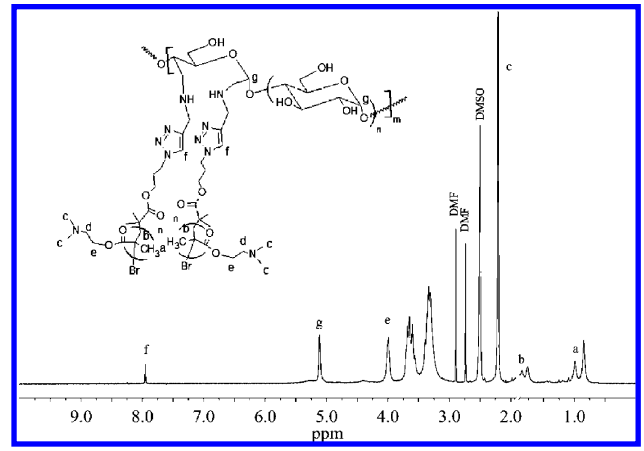

Figure 6. ^{1}H NMR (300 MHz, DMSO-d_6/H_2O 100/1, 60 °C) of the AmDMAE copolymer.

PBA-N_3 and an alkynyl-functionalized branched glucan well-soluble in DMF. For that purpose, the following parameters had been varied: (a) Cu(I)/reactive groups ratio, (b) reaction solvent, and (c) reaction temperature. Quantitative PBA-N_3 grafting was observed to require an equimolar amount of catalyst with respect to the alkyne groups, only partial grafting being achieved with a lower catalyst amount. We observed a similar effect by replacing some of the DMF with water; the lower conversion being ascribed in this case to the consequent heterogeneity of the system. Changing the reaction temperature in the 40−60 °C range did not significantly influence the grafting yield. To understand the quite higher catalyst amount requirement than that in cycloadditions involving low-molecular-weight species (0.01 to 0.1 equiv of catalyst),[33,36,66] we must consider some specific characteristics of polysaccharide systems under investigation. These are the very low concentration of the functional groups (typically 10^{-3} to 10^{-4} mol L^{-1}), the possible capture of some copper(I) by complexation with the numerous hydroxyl groups, and the molecular or supramolecular steric hindrance.

The weight loss curve recorded from the TGA analysis of the AmBA graft copolymer (Figure 5) showed two well-resolved degradation steps, thus allowing the quantitative evaluation of its composition (Table 2). For this purpose, the peak integrals in the weight-loss first derivative curve from the thermograms of the copolymer and of the grafting parent polymers Am-PA and PBA-N_3 were considered, and the fractional weight loss attributed to the acrylic chains was calculated accordingly. The amount of PBA in AmBA was found to be 39 wt %, which corresponds to an almost quantitative grafting yield (95 wt % with respect to the amount of PBA-N_3 in the reaction feed). Accordingly, no acrylic homopolymer could be detected in the washing solvent, the efficiency of the proposed click promoted grafting "onto" strategy for the preparation of comb like copolymers being thus confirmed.

The same conditions as those used for the AmBA preparation were adopted in the grafting of PBMA and PDMAEMA chains onto amylose (AmBMA and AmDMAE, respectively, Table 3). In the case of PBMA, the only difference in the synthetic procedure was the amount of azido-end-functionalized grafting polymer PBMA-N_3, fed in a higher ∼80 mol % with respect to the alkynyl groups on amylose as compared with the much smaller ∼0.33 mol % used in the synthesis of AmBA. However, the grafting yield was again almost quantitative (91 wt %), thus indicating the possibility of tuning the amount of grafted chains up to the complete conversion of alkynyl groups on amylose. In an attempt to simplify the reaction conditions, only DMF was used instead of DMSO/DMF mixed solvent in run AmBMA2, and the reaction temperature was set to 40 °C (Table 2). As a result, the reaction was carried out in suspension, and a lower 63 wt % grafting yield was obtained. Similarly, in the synthesis of AmHMA, an incomplete solubility of the grafting poly(hexyl methacrylate) resulted in a poor 30 wt % grafting yield achieved after 6 days of reaction. The above results showed the importance of having both reactants well-solubilized in the reaction medium to achieve quantitative grafting.

When the functional PDMAEMA-N_3 was used as the grafting polymer, the result of the TGA analysis performed on the reaction product AmDMAE indicated quantitative grafting onto amylose (Table 2), and the ^{1}H NMR spectrum (Figure 6) showed the presence of the typical resonances from both amylose and synthetic polymer, both results confirming the effectiveness of the adopted grafting conditions also when using functional polymethacrylates. Integration of the resonance peaks gave values in agreement with the copolymer composition from TGA data analysis, this being an evidence of the good solubility of the copolymer in the solvent used for the spectroscopic analysis. A 4.5 mol % grafted PDMAEMA chains per pyranoside unit was calculated from the ratio between the resonance integrals of the triazole proton at 7.95 ppm and of the anomeric proton of the pyranose ring at 5.11 ppm. Such a grafting density is in good agreement with the functionalization degree of amylose by alkynyl groups (Table 3), thus confirming the quantitative conversion of the alkynyl groups to grafted chains.

Self-Assembling and Nanoparticle Morphology of Grafted Copolymers. A preliminary investigation on the behavior of the amphiphilic graft copolymers in water showed their aqueous solution to be almost completely transparent at concentrations of amylose-based copolymers <1 g/L. DLS analysis performed on the aqueous graft copolymers always showed detectable scattered intensity except in the case of AmDMAE, which was therefore regarded as fully soluble. The presence of nanoparticles in all other samples suggested by the light scattering experiments was confirmed by the TEM observations, showing the presence of nanoparticles <100 nm (Figure 7). Cumulant analysis of the DLS data from unfiltered or not centrifuged dispersions of AmBA, AmBMA, and AmHMA always showed the presence of both small (<100 nm) and large (≥350 nm) nanoparticles (Table 4). The total scattered intensity decreased after filtration or centrifugation because of the removal of the larger particle or particle aggregate families (ΔCR, Table 4). In fact, the TEM micrographs of Figure 7c,d show the presence of aggregates of spheroidal particles with well-defined size in the 30−40 nm

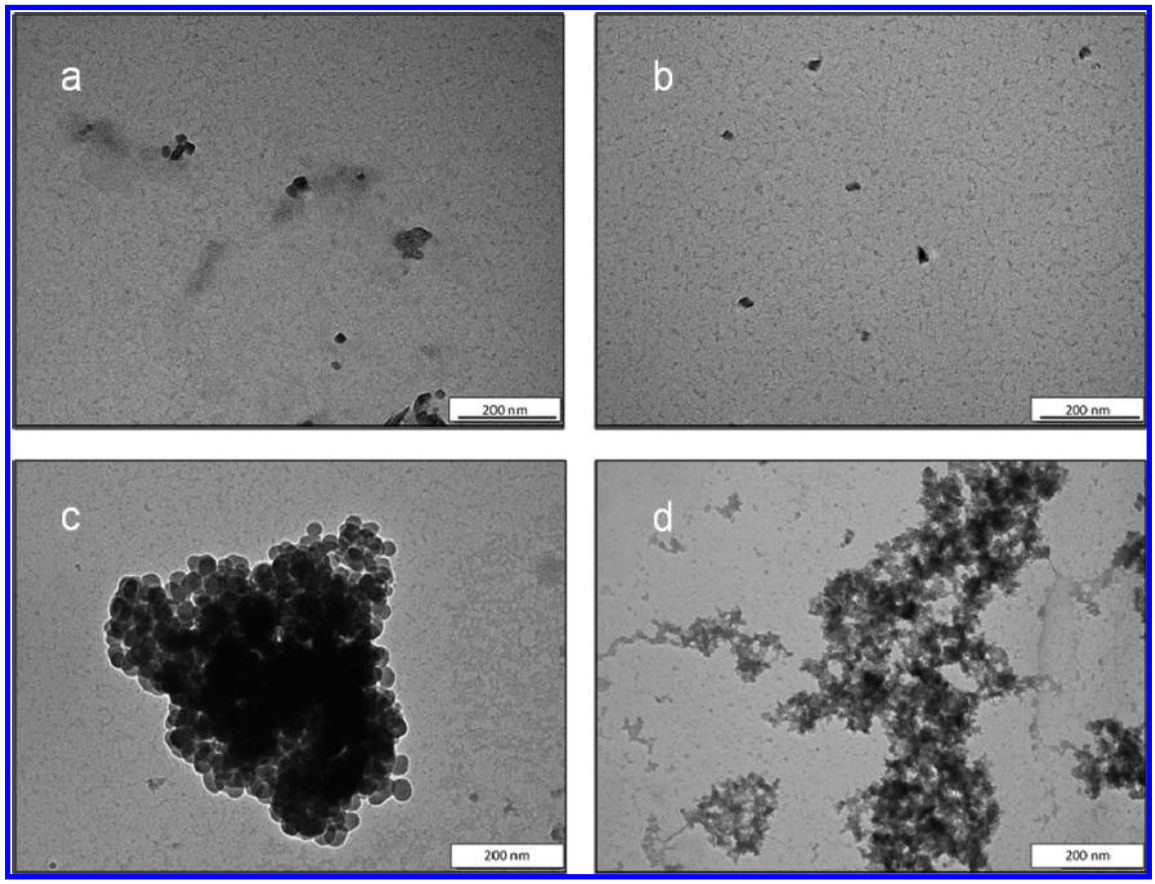

Figure 7. TEM micrographs of nanoparticles from (a,b) filtered and (c,d) unfiltered 1 g/L aqueous dispersions of (a,c) AmBMA and (b,d) AmBA. Dispersions obtained by solvent exchange dialysis from DMSO solutions at 2 g/L.

Table 4. Average Diameter of Amylose Copolymer Nanoparticles in Water (concn = 1 g/L) from DLS Measurement (Dispersions Obtained by Solvent Exchange Dialysis from DMSO Solutions at 2 g/L)

sample	note[a]	Δ(CR)[b]	hydrodynamic diameter (D_H) (nm)[c]	particles > 350 nm (vol %)
AmBMA			46 ± 6	13.0
	centrifuged	21	45 ± 4	
	filtered	47	31 ± 2	
AmBA			27 ± 3	13.5
	centrifuged	37	24 ± 3	10.0
	filtered	77	30 ± 3	
AmHMA			41 ± 4	16.0
	centrifuged	26	29 ± 2	
	filtered	43	26 ± 2	

[a] Centrifuged samples were processed at 4400 RCF for 10 min; filtered samples were processed through 0.45 μm cellulose acetate syringe filters. [b] $\Delta(CR) = [(CR) - (CR)_T]*100/(CR)$, where (CR) = count rate of as prepared dispersion, $(CR)_T$ = count rate of centrifuged or filtered dispersion. [c] Weighed intensity average of the most abundant smaller sized particle family.

range in the case of AmBMA, whereas undefined morphologies apparently consisting of much smaller flocculated particles of irregular shape were observed with the PBA and PHMA derivatives. To explain such differences, one should take into account the fact that the two latter polymers have glass-transition temperatures that are much lower than those of PBMA (PBA = −51.5 °C; PHMA = −4.2 °C; PBMA = +26.0 °C), resulting in corresponding copolymers with high macromolecular mobility and tendency toward interparticle coalescence on drying. Actually, the low molecular weight of the grafted chains, which is below the entanglement length[67] for all investigated copolymers (Table 1), does not favor micelle clustering in solution but cannot prevent coalescence of particles during the preparation of samples for TEM analysis from relatively concentrated dispersions.

Heterogeneity of both unfiltered and 0.45 μm filtered aqueous solutions of AmBMA, for instance, is evident by comparing the respective scattered light intensity profiles. The larger aggregates contribute to the scattered intensity mainly at small scattering angle (due to the form factor), and only the filtering with 0.2 μm pore size significantly decreases such heterogeneity. (See Figure 8.)

The dependence of dynamic and static light scattering on the scattering angle θ can add more information on the particle morphology. In Figure 9 is shown the decay or relaxation rate Γ, as obtained from the normalized scattered electric field autocorrelation function for the AmBMA copolymer by a second-order cumulant expansion. The average translational diffusion coefficient D, that is, the average value from a monomodal polydisperse particle size distribution (resulting in a distribution of decay rates $\Gamma = DQ^2$ of monodisperse scatterers assumed as rigid spheres, where Q is the exchanged wavevector of the autocorrelation function), can be measured below Q = 20 μm^{-1}, whereas above this value, the onset of the internal motions regime occurs. The diffusion coefficient does not seem to depend on the concentration of the aqueous copolymer solution (data not shown) at the lowest concentration values (0.1 to 0.01 g/L), indicating that interparticle interactions can be neglected. Under this condition, the Einstein−Stokes relation $R_H = k_B T/(6\pi\eta D)$ (where k_B is the Boltzmann's constant, T is the absolute temperature, and η is the solvent viscosity) can be applied, giving an average hydrodynamic radius of R_H = 48 ± 2 nm for AmBMA. The crossover at $QR_H \approx 1$ between

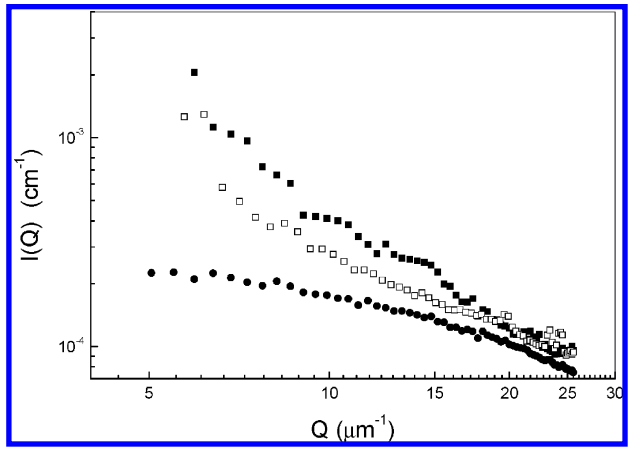

Figure 8. Scattered intensity profile of the AmBMA/water dispersion at 0.1 g/L before (■) and after the filtering procedure with 0.45 (□) and 0.2 μm (●) pore size cellulose acetate filters (dispersions obtained by solvent exchange dialysis from DMSO solutions at 20 g/L). The scattering intensity wave vector scales with the scattering angle θ as $Q = (4\pi n/\lambda)\sin\vartheta$.

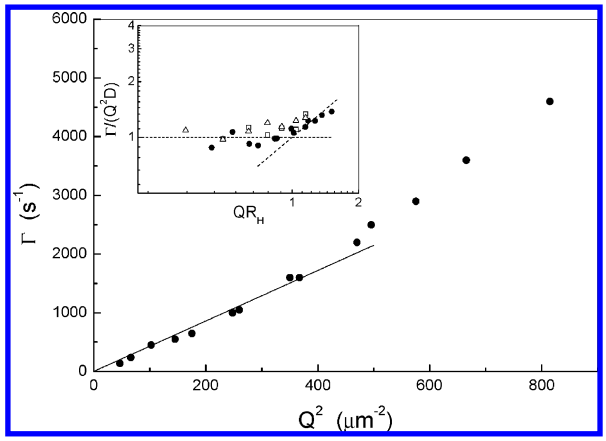

Figure 9. Correlation functions decay rate of the filtered aqueous solution of AmBM2A at 0.1 g/cm^3 (dispersions obtained by solvent exchange dialysis from DMSO solutions at 20 g/L). The straight line is the linear fit in the Q range below 20 μm^{-1}. In the inset, the normalized decay rate is reported at different concentration values: $c = 0.01$ (□), 0.1 (●), and 1 g/cm^3 (△). The two dashed straight lines represent the regions in which Γ is proportional to Q^2 and Q^3, respectively.

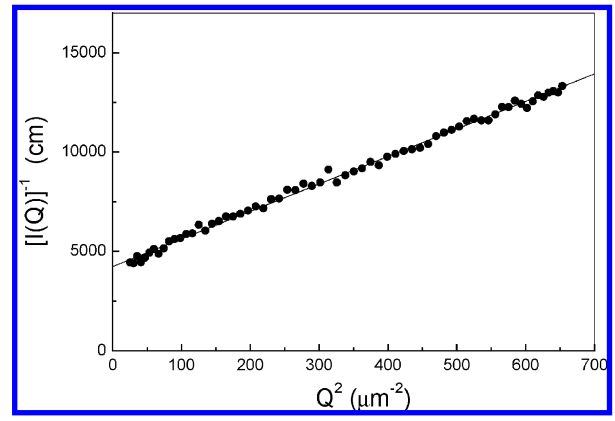

Figure 10. Reciprocal of the excess scattered intensity $I(Q)$ of the filtered aqueous solution of AmBMA at 0.1 g/cm^3 (dispersions obtained by solvent exchange dialysis from DMSO solutions at 20 g/L). Excess scattered intensity determined from static light scattering measurements and proportional, at high dilution, to the form factor. The continuous line is the fit according to the Ornstein−Zernike equation.

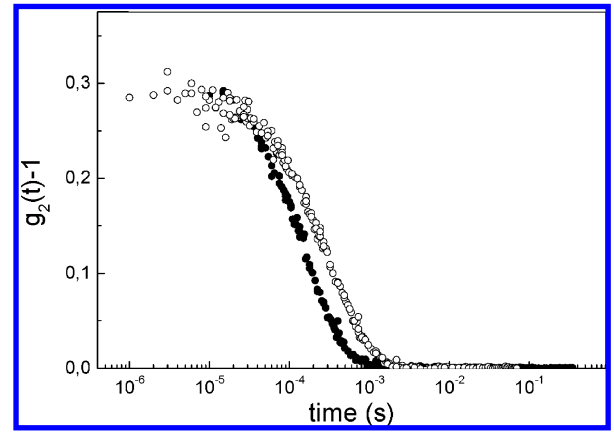

Figure 11. Comparison between the scattered intensity autocorrelation function of AmBMA at 0.1 g/L obtained by solvent exchange dialysis from DMSO solutions at 20 (○) and 2 g/L (●).

translational diffusion and internal motions is displayed more clearly in the inset of Figure 9, in which the results for all investigated concentrations indicate that the aggregates are not rigid.

The scattered intensity profile can be fitted with the Ornstein−Zernike equation (Figure 10), describing particles with nonhomogeneous internal density distribution and correlation length ξ. By taking as the radius of gyration of the aggregate $R_g = \sqrt{3}\xi$, the obtained value for AmBMA was $R_g \approx 95$ nm. Both the form factor of the aggregates, indicated by the Ornstein−Zernike profile, and the R_g/R_H ratio suggest that the mass of the aggregates is not homogeneously distributed in the occupied volume. This result is consistent with the formation of micellar clusters.

When the aqueous dispersions were prepared starting from less-concentrated DMSO solutions (2 instead of 20 g/L), smaller values of the average particle size were observed from the cumulant analysis (Figure 11). In particular, R_H was 25 ± 1 nm for AmBMA filtered with a 0.2 μm filter. It is worth pointing out that the slightly lower average value reported in Table 4 ($D_H/2 \approx 16$ nm for the filtered AmBMA) is referred to the singled out family of particles in the smaller size range. Moreover, the measured particle size was not affected by dilution, even when starting from 1 g/L aqueous solutions, an indication of the achievement of more stable particle morphology, differently from the case of the dispersions prepared starting from the 20 g/L DMSO solution.

This sample preparation method, that is, solvent exchange by dialysis starting from 2 g/L DMSO solutions, was thus adopted to compare the average particle size of samples AmBA, AmHMA, and AmBMA at 90° scattering angle. At least a bimodal particle distribution was observed in all samples, with the smallest particle family listed in Table 4 as the most abundant both before and after filtration or centrifugation. In fact, the number fraction of the particles belonging to the largest families was negligible under all experimental conditions, although the same did not always hold true for the volume fraction. The hydrodynamic particle diameter for the most abundant distribution was centered at ~30 nm for all three filtered dispersions of amylose graft copolymers. Therefore, it must be assumed that the different grafted chains give a similar contribution to the hydrophobic character of the graft copolymer. In particular, the slightly smaller average size displayed by AmHMA suggests a more pronounced hydrophobic contribution from the PHMA grafted chains, leading to the formation of

amphiphilic copolymer assemblies with a denser hydrophobic core. Accordingly, the Hildebrand solubility parameters (δ) of the three synthetic homopolymers are rather similar: δ(PBA) = 19.7; δ(PBMA) = 19.1; δ(PHMA) = 18.8; and $\delta(H_2O)$ = 48.0 $[MPa]^{1/2}$.[68]

Conclusions

The results obtained in the grafting "onto" experiments evidenced that the Cu(I) catalyzed azide−alkyne [3 + 2]-dipolar cycloaddition ("click") is an efficient and versatile procedure for the hydrophobic modification of amylose, opening the way to the synthesis of well-defined hybrid polysaccharide structures with advanced functional properties. The oxidation-reductive amination reaction sequence was shown to be an easy and efficient method for functionalizing polysaccharides with alkynyl groups under mild reaction conditions involving moderate heating in air, with conservation of the macromolecular chain. It is expected that the main drawback of a moderate yield in the reductive amination stage will be overcome by further research work. One important feature of the "click" grafting of polymeric chains onto the modified polysaccharide is that it can be conveniently exploited for the synthesis of graft copolymers with tunable grafting degree. Indeed, this last parameter can be controlled in different ways, such as by varying the fractional amount of grafting chains in the reaction feed or by using a polysaccharide with different content of alkynyl groups.

The versatility of the proposed procedure was confirmed through the successful synthesis of graft copolymers using different grafting chains, namely, PBA, PBMA, PHMA, and PDMAEMA.

The obtained graft copolymers were shown to self-assemble into nanoparticle aggregates in water when the grafted synthetic polymer chains were sufficiently hydrophobic to make the hybrid copolymer amphiphilic.

Acknowledgment. We wish to thank Professor Francesco Ciardelli (University of Pisa, Italy) and Professor Nicola Tirelli (University of Manchester, U.K.) for helpful discussions and suggestions.

Supporting Information Available. Details of the light scattering data analysis procedure; synthesis and spectroscopy characterization of 2-bromo-isobutyric acid 3-azidopropylester (BiBAP) and ethyl-2-azidobutyrate. This material is available free of charge via the Internet at http://pubs.acs.org.

References and Notes

(1) Kataoka, K.; Harada, A.; Nagasaki, Y. *Adv. Drug Delivery Rev.* **2001**, *47*, 113–131.
(2) Savic, R.; Luo, L. B.; Eisenberg, A.; Maysinger, D. *Science* **2003**, *300*, 615–618.
(3) Bae, Y.; Nishiyama, N.; Kataoka, K. *Bioconjugate Chem.* **2007**, *18*, 1131–1139.
(4) Jabr-Milane, L.; Vlerken, L.; Devalapally, H.; Shenoy, D.; Komareddy, S.; Bhavsar, M.; Amiji, M. *J. Controlled Release* **2008**, *130*, 121–128.
(5) Zhang, L.; Lin, J.; Lin, S. *J. Phys. Chem. B* **2007**, *111*, 9209–9217.
(6) Cansell, M.; Parisel, C.; Jozefonvicz, J.; Letouneur, D. *J. Biomed. Mater. Res.* **1999**, *44*, 140–148.
(7) Francis, M.; Lavoie, L.; Winnik, F.; Leroux, J. C. *Eur. J. Pharm. Sci.* **2003**, *56*, 337–346.
(8) Na, K.; Lee, T. B.; Park, K.-H.; Shin, E.-K.; Lee, Y.-B.; Choi, H.-K. *Eur. J. Pharm. Sci.* **2003**, *18*, 165–173.
(9) Liu, Z.; Jiao, Y.; Wang, Y.; Zhou, C.; Zhang, Z. *Adv. Drug Delivery Rev.* **2008**, *60*, 1650.
(10) Bhattacharya, A.; Misra, B. N. *Prog. Polym. Sci.* **2004**, *29*, 767–814.
(11) Borner, H. G.; Matyjaszewski, K. *Macromol. Symp.* **2002**, *177*, 1–15.
(12) Zhao, B.; Brittain, W. J. *Prog. Polym. Sci.* **2000**, *25*, 677–710.
(13) Kaneko, Y.; Matsuda, S.-I.; Kadokawa, J.-I. *Biomacromolecules* **2007**, *8*, 3959–3964.
(14) Appelhans, D.; Komber, H.; Quadir, M. A.; Richter, S.; Schwarz, S.; van der Vlist, J.; Aigner, A.; Müller, M.; Loos, K.; Seidel, J.; Arndt, K.-F.; Haag, R.; Voit, B. *Biomacromolecules* **2009**, *10*, 1114–1124.
(15) Roy, D.; Semsarilar, M.; Guthrie, J. T.; Perrier, S. *Chem. Soc. Rev.* **2009**, *38*, 2046–2064.
(16) Jenkins, D. W.; Hudson, S. M. *Chem. Rev.* **2001**, *101*, 3245–3273.
(17) Zampano, G.; Bertoldo, M.; Bronco, S. *Carbohydr. Polym.* **2009**, *75*, 22–31.
(18) Bledzki, A. K.; Gassan, J. *Prog. Polym. Sci.* **1999**, *24*, 221–274.
(19) Mansson, P.; Westfelt, L. *J. Polym. Sci., Polym. Chem.* **1981**, *19*, 1509–1515.
(20) Tsubokawa, N.; Iida, T.; Takayama, T. *J. Appl. Polym. Sci.* **2000**, *75*, 515–522.
(21) Mourya, V. K.; Inamdar, N. N. *React. Funct. Polym.* **2008**, *68*, 1013–1051.
(22) Bhattarai, N.; Matsen, F. A.; Zhang, M. *Macromol. Biosci.* **2005**, *5*, 107–111.
(23) Liu, L.; Li, F.; Guo, S. *Macromol. Biosci.* **2006**, *6*, 855–861.
(24) Karakasyan, C.; Lack, S.; Brunel, F.; Maingault, P.; Hourdet, D. *Biomacromolecules* **2008**, *9*, 2419–2429.
(25) Bokias, G.; Mylonas, Y.; Staikos, G.; Bumbu, G. G.; Vasile, C. *Macromolecules* **2001**, *34*, 4958–4964.
(26) Houdet, D.; L'Alloret, F.; Audebert, R. *Polymer* **1997**, *38*, 2535–2547.
(27) Cho, K. Y.; Chung, T. W.; Kim, B. C.; Kim, M. K.; Lee, J. H.; Wee, W. R.; Cho, C. S. *Int. J. Pharm.* **2003**, *24*, 83–90.
(28) Fleury, E.; Tizzotti, M.; Destarac, M.; Labeau, M.-P.; Hamaide, T.; Drockenmuller, E. Patent WO2009063082 A1 - 2009-05-22.
(29) Tizzotti, M.; Creuzet, C.; Labeau, M.-P.; Hamaide, T.; Boisson, F.; Drockenmuller, E.; Charlot, A.; Fleury, E. *Macromolecules* **2010**, *43*, 6843–6852.
(30) Tankam, P. F.; Müller, R.; Mischnick, P.; Hopf, H. *Carbohydr. Res.* **2007**, *342*, 2049–2060.
(31) Liebert, T.; Hänsch, C.; Heinze, T. *Macromol. Rapid Commun.* **2006**, *27*, 208–213.
(32) Mortisen, D.; Peroglio, M.; Alini, M.; Aglin, D. *Biomacromolecules* **2010**, *11*, 1261–1272.
(33) Crescenzi, V.; Cornelio, L.; Di Meo, C.; Nardecchia, S.; Lamanna, R. *Biomacromolecules* **2007**, *8*, 1844–1850.
(34) Yuan, W.; Zhao, Z.; Gu, S.; Ren, J. *J. Polym. Sci., Polym. Chem.* **2010**, *48*, 3476–3486.
(35) Hasegawa, T.; Umeda, M.; Numata, M.; Fujisawa, T.; Haraguchi, S.; Sakurai, K.; Shinkai, S. *Chem. Lett.* **2006**, *35*, 82–83.
(36) Hasegawa, T.; Umeda, M.; Numata, M.; Li, C.; Bae, A. H.; Fujisawa, T.; Haraguchi, S.; Sakuraib, K.; Shinkai, S. *Carbohydr. Res.* **2006**, *341*, 35–40.
(37) Numata, M.; Okumura, S.; Kimura, T.; Sakurai, K.; Shinkai, S. *Org. Biomol. Chem.* **2007**, *5*, 2404–2412.
(38) Pohl, M.; Schaller, J.; Meister, F.; Heinze, T. *Macromol. Rapid Commun.* **2008**, *29*, 142–148.
(39) Hafrén, J.; Zou, W.; Córdova, A. *Macromol. Rapid Commun.* **2006**, *27*, 1362–1366.
(40) Bernard, J.; Save, M.; Arathoon, B.; Charleux, B. *J. Polym. Sci., Polym. Chem.* **2008**, *46*, 2845–2857.
(41) Zampano, G.; Bertoldo, M.; Ciardelli, F. *React. Funct. Polym.* **2010**, *70*, 272–281.
(42) Iha, R. K.; Wooley, K. L.; Nystrom, A. M.; Burke, D. J.; Kade, M. J.; Hawker, C. J. *Chem. Rev.* **2009**, *109*, 5620–5686.
(43) Binder, W. H.; Sachsenhofer, R. *Macromol. Rapid Commun.* **2007**, *28*, 15–54.
(44) Binder, W. H.; Sachsenhofer, R. *Macromol. Rapid Commun.* **2008**, *29*, 952–981.
(45) Lodge, T. P. *Macromolecules* **2009**, *42*, 3827–3829.
(46) Bao, H.; Li, L.; Gan, L. H.; Ping, Y.; Li, J.; Ravi, P. *Macromolecules* **2010**, *43*, 5679–5687.
(47) Braunecker, W. A.; Brown, W. C.; Morelli, B. C.; Tang, W.; Poli, R.; Matyjaszewski, K. *Macromolecules* **2007**, *40*, 8576–8585.
(48) Ehrenfreund-Kleinmana, T.; Gazit, Z.; Gazit, D.; Azzam, T.; Golenser, J.; Domb, A. J. *Biomaterials* **2002**, *23*, 4621–4631.
(49) Eliyahu, H.; Siani, S.; Azzam, T.; Domb, A. J.; Barenholz, Y. *Biomaterials* **2006**, *27*, 1646–1655.
(50) Azzam, T.; Eliyahu, H.; Shapira, L.; Linial, M.; Barenholz, Y.; Domb, A. J. *J. Med. Chem.* **2002**, *45*, 1817–1824.
(51) Azzam, T.; Raskin, A.; Makovitzki, A.; Brem, H.; Vierling, P.; Lineal, M.; Domb, A. J. *Macromolecules* **2002**, *35*, 9947–9953.

(52) Wu, M.; Kuga, S. *J. Appl. Polym. Sci.* **2006**, *100*, 1668–1672.
(53) Loos, K.; Müller, A. H. E. *Biomacromolecules* **2002**, *3*, 368–373.
(54) Bosker, W. T. E.; Agoston, K.; Stuart, M. A. C.; Norde, W.; Timmermans, J. W.; Slaghek, T. M. *Macromolecules* **2003**, *36*, 1982–1987.
(55) Janciauskaite, U.; Rakutyte, V.; Miskinis, J.; Makuska, R. *React. Funct. Polym.* **2008**, *68*, 787–796.
(56) Zhao, H.; Heindel, N. D. *Pharm. Res.* **1991**, *8*, 400–402.
(57) Villari, V.; Micali, N. *J. Pharm. Sci.* **2008**, *97*, 1703–1730.
(58) Arecchi, F. T.; Corti, M.; Degiorgio, V.; Donati, S. *Opt. Commun.* **1971**, *3*, 284–288.
(59) Gong, Q.; Wang, L.-Q.; Tu, K. *Carbohydr. Polym.* **2006**, *64*, 501–509.
(60) Coessens, V.; Nakagawa, Y.; Matyjaszewski, K. *Polym. Bull.* **1998**, *40*, 135–142.
(61) Jiang, X.; Lok, M. C.; Hennink, W. E. *Bioconjugate Chem.* **2007**, *18*, 2077–2084.
(62) Agut, W.; Taton, D.; Lecommandoux, S. *Macromolecules* **2007**, *40*, 5653–5661.
(63) Lowe, A. B.; Wang, R. *Polymer* **2007**, *48*, 2221–2230.
(64) Lane, C. F. *Synthesis* **1975**, *1975*, 135–146.
(65) Golas, P. L.; Tsarevsky, N. V.; Sumerlin, B. S.; Matyjaszekski, K. *Macromolecules* **2006**, *39*, 6451–6457.
(66) Schatz, C.; Louguet, S.; Le Meins, J.-F.; Lecommandoux, S. *Angew. Chem., Int. Ed.* **2009**, *48*, 2572–2575.
(67) Zosel, A.; Ley, G. *Macromolecules* **1993**, *26*, 2222–2227.
(68) Bicerano, J. *Prediction of Polymer Properties*, 2nd ed.; Marcel Dekker: New York, 1996; pp 126−130.

BM101143Q